SCIENTIFIC REPORTS

There are amendments to this paper

OPEN

SUBJECT AREAS:
SYSTEMS BIOLOGY
MEDICAL RESEARCH

Received
26 November 2013

Accepted
29 January 2014

Published
24 February 2014

Correspondence and requests for materials should be addressed to Z.Y.L. (lizhiyan112013@163.com) or N.L. (linna888@163.com)

* These authors contributed equally to this work.

A systems biology-based investigation into the therapeutic effects of Gansui Banxia Tang on reversing the imbalanced network of hepatocellular carcinoma

Yanqiong ZHANG[1]*, Xiaodong GUO[2]*, Danhua WANG[1], Ruisheng LI[2], Xiaojuan LI[2], Ying XU[1], Zhenli LIU[3], Zhiqian SONG[3], Ya LIN[1], Zhiyan LI[2] & Na LIN[1]

[1]Institute of Chinese Materia Medica, China Academy of Chinese Medical Sciences, Beijing 100700, China, [2]302 Hospital of PLA, Beijing 100039, China, [3]Institute of Basic Theory, China Academy of Chinese Medical Sciences, Beijing 100700, China.

Several complex molecular events are involved in tumorigenesis of hepatocellular carcinoma (HCC). The interactions of these molecules may constitute the HCC imbalanced network. Gansui Banxia Tang (GSBXT), as a classic Chinese herbal formula, is a popular complementary and alternative medicine modality for treating HCC. In order to investigate the therapeutic effects and the pharmacological mechanisms of GSBXT on reversing HCC imbalanced network, we in the current study developed a comprehensive systems approach of integrating disease-specific and drug-specific networks, and successfully revealed the relationships of the ingredients in GSBXT with their putative targets, and with HCC significant molecules and HCC related pathway systems for the first time. Meanwhile, further experimental validation also demonstrated the preventive effects of GSBXT on tumor growth in mice and its regulatory effects on potential targets.

Hepatocellular carcinoma (HCC) is one of the most common malignant tumors with an increasing incidence and the third leading cause of cancer-related deaths worldwide[1]. The distribution of HCC is unbalanced throughout the world, with the highest incidence in Asia and Sub-Saharan Africa, especially in China[2]. As a notoriously aggressive solid tumor, HCC is characterized by fast infiltrating growth, early metastasis, high-grade malignancy, and poor prognosis. This cancer often develops as a consequence of underlying liver diseases such as hepatitis B virus (HBV) and hepatitis C virus (HCV) infections, and is almost associated with cirrhosis[3]. At present, surgical hepatic resection and liver transplantation are the only curative treatment modality to confer survival benefit in HCC patients. However, the resistance of HCC to existing treatments and the lack of biomarkers for early detection make it one of the most hard-to-treat cancers. The overall 5-year survival rate for HCC patients is still only 5%[4]. Since HCC remains incurable with current therapies, novel therapeutic agents or strategies are urgently needed.

Traditional Chinese Medicine (TCM), as one of the most popular complementary and alternative medicine modalities worldwide, has been practiced in China for more than 2,000 years. TCM emphasize on regulating the integrity of the human body as well as the interaction between human individuals and their environment, which is the balance-regulation theory[5]. Several complex molecular events have been demonstrated to be involved in human tumorigenesis. The interactions of these abnormal molecules may constitute cancer-specific imbalanced networks. TCM, which efficiently reverse the cancer-specific imbalanced networks, has become an available option in many cancer centers in Asia[6], Western countries[7], and Africa[8]. Accumulating studies have demonstrated that Chinese herbs have an anticancer effect by inducing apoptosis of cancer cells, enhancing the immune system, inducing cell differentiation, and inhibiting telomerase activities and growth of tumor[9]. In the treatment of HCC, TCM can stimulate host immune response that has cytotoxic activity against tumor cells[10]. For example, several TCM ingredients, such as Panax ginseng, toad skin secretions (bufotoxin), Astragalus, beetle extracts (Mylabris), Atractylodes, Curcuma and Bupleurum, have been reported to have oncologic and immunologic

pharmacology[11]. Gansui Banxia Tang (GSBXT), as a classic TCM formula from Chinese medical sage Zhang Zhongjing is prepared from a basic formula of five ingredients, including Radix Kansui (Gansui), Rhizoma Pinelliae (Banxia), Radix Glycytthizae (Gancao), Raidix Paeoniae Alba (Baishao) and Mel (Fengmi). It is widely produced in China in accordance with the China Pharmacopoeia standard of quality control. In TCM theory, multiple agents contained in one formula must work synergistically. With regard to GSBXT, Radix Kansui and Rhizoma Pinelliae are the primary ingredients and are believed to be strongly effective in expelling water; Raidix Paeoniae Alba, Radix Glycytthizae and Mel can either focus the actions of the formula on a certain area of the body or harmonize and integrate the actions of the other ingredients of the formula. Since it contains one of "Eighteen antagonisms"-the controversial prohibited combinations in TCM, namely Radix Kansui (Gansui) and Radix Glycytthizae (Gancao), the clinical applications of GSBXT have been hampered. This formula has been used for the treatment of cancerous ascites, pleural effusion, peritoneal effusion, pericardial effusion, cranial cavity effusion, intestinal tuberculosis, gastrointestinal inflammation, and several types of cancers, such as HCC and esophageal cancer[12–19]. However, its pharmacological mechanisms have not been fully elucidated.

Chinese herbal formulas (Fu-Fang) are multi-component and multi-target agents, essentially achieving the therapeutic effectiveness through collectively modulating the molecular network of the body system using its active ingredients. System biology, with its extremely high efficiency and molecular level representation, has been widely used in understanding the complex interactions of proteins and small molecules in a biological system and evaluating how these interactions give rise to the function and behavior of that system. It provides powerful new tools and conceptions to measure the efficacy and to reveal the functional mechanisms of drugs, especially the multi-target drugs. In our previous study[20], we developed a systems-pharmacological model by combining multiple drug-target prediction and network pharmacology strategies, to investigate the pharmacological mechanisms of Wu Tou Tang acting on rheumatoid arthritis for the first time. Since network description and analysis can give a systems-level understanding of drug action and disease complexity[21], the combination of special disease related network using disease significant molecules into the systems-pharmacological model will be very helpful to explain the functions of herbal medicines on special diseases. Thus in this study, we developed a comprehensive systems approach for understanding the pharmacological mechanisms of GSBXT acting on HCC. Our protocol includes four main steps: (1) prediction of putative targets for GSBXT; (2) collection of HCC significant molecules and construction of HCC imbalanced network; (3) investigation on the relationships of putative targets of GSBXT with HCC imbalanced network and relative signal pathways, which offers a great opportunity for the deep understanding of the pharmacological mechanisms of GSBXT on reversing this disease-specific imbalanced network; (4) experimental validation of the effects of GSBXT on the growth of HCC and its candidate targets for HCC treatment by the nude mouse xenograft assays. Figure 1 depicts the flowchart of the whole experimental procedure.

Results & Discussion

Putative targets for GSBXT. Based on our previous developed target prediction system[20], 117 similar drugs of chemical components and 53 known targets of these similar drugs as putative targets for GSBXT were identified. As shown in Table 1, the 40 chemical components yielded 53 putative targets and the connections between them reach up to 161. The amount of putative targets hit by Radix Glycytthizae, Radix Kansui, Raidix Paeoniae Alba, Mel and Rhizoma Pinelliae were 38, 13, 12, 9 and 1, respectively. There is a significant target overlap between Radix Glycytthizae and Radix Kansui (11 putative targets), while Rhizoma Pinelliae had no common putative targets with Radix Glycytthizae, Radix Kansui, Mel, and Raidix Paeoniae Alba. Please see detailed information on putative targets and corresponding chemical components of five ingredients in GSBXT in Supplementary Table S1. Interestingly, 25 in 53 putative targets of GSBXT were HCC significant proteins. Among them, 15 were candidate HCC targets, suggesting the possible role of this formula in the treatment of HCC.

Identification of candidate protein targets associated with HCC therapy. In total, 6179 HCC significant genes and 977 HCC significant proteins which were differentially expressed or had genetic variations in HCC tissues relative to their corresponding normal tissues were collected from five existing HCC related databases (OncoDB.HCC, HCC.net, dbHCCvar, EHCO and Liverome) after removing redundancy. Since multiple biological processes or pathways are implicated in tumorigenesis and tumor progression of HCC, we constructed HCC imbalanced network using PPI information between HCC significant proteins and other human proteins. This network consists of 10,894 nodes and 122,181 edges. According to the previous study of Li et al.[22], we identified a node as a hub protein if its degree is more than 2 fold of the median degree of all nodes in a network. As the results, there are 2098 hub HCC significant proteins. The network of hub HCC significant proteins consists of 2098 nodes and 61,143 edges. Four topological features, 'Degree,' 'Betweenness', 'Closeness' and 'K value' (defined in 'Materials and methods' section), were chosen to identify candidate HCC targets. After calculating the value of the four features for each hub HCC significant protein in the PPI network, the median values of 'Degree', 'Betweenness', 'Closeness' and 'K value' were 67, 0.03, 39.37 and 31, respectively. Therefore, we determined that HCC significant proteins with 'Degree' $>$ 67, 'Betweenness' $>$ 0.03, 'Closeness' $>$ 39.37, and 'K value' $>$ 31 were candidate HCC targets for tumor therapy. As a result, 331 proteins were identified as candidate HCC targets. Please see detailed information on topological features of these candidate HCC targets in Supplementary Table S2. According to the results of enrichment analysis based on GO annotation system and KEGG pathway in Supplementary File S1 and Figure S1, these candidate HCC markers were more frequently involved in cellular protein metabolic process, translational elongation and intracellular signaling cascade, which are associated with cancer development and metastasis.

Identification of the underlying pharmacological mechanisms of GSBXT acting on HCC. In order to shed light on the synergistic effects and pharmacological mechanisms of GSBXT acting on HCC, we have constructed the ingredient-chemical component-putative target network, putative target PPI network, and ingredient-major putative target-candidate HCC target network.

Ingredient-chemical component-putative target network for GSBXT. We firstly constructed the Ingredient-chemical component-putative target network for GSBXT in order to clarify the relationships between the ingredients and corresponding putative targets. As shown in Figure 2, the network consists of 98 nodes (5 ingredients, 40 chemical components and 53 putative targets) and 201 edges. The mean number of putative targets per chemical components was 1.33. Among 40 chemical components, 6 have high degree distributions and each of them hits 11 putative targets. Five of them come from Radix Glycytthizae, such as Isogosferol, licochalcone_A, Neohancoside_A, Neoisopulegol, Phebalosin, and the other one (euponin) come from Radix Kansui. Since the chemical components with higher degree in the network have been demonstrated to be more pharmacologically important and our data mentioned above showed that Radix Kansui shared the most common targets with Radix Glycytthizae, Radix Kansui and Radix Glycytthizae might be major ingredients in this pharmacological network.

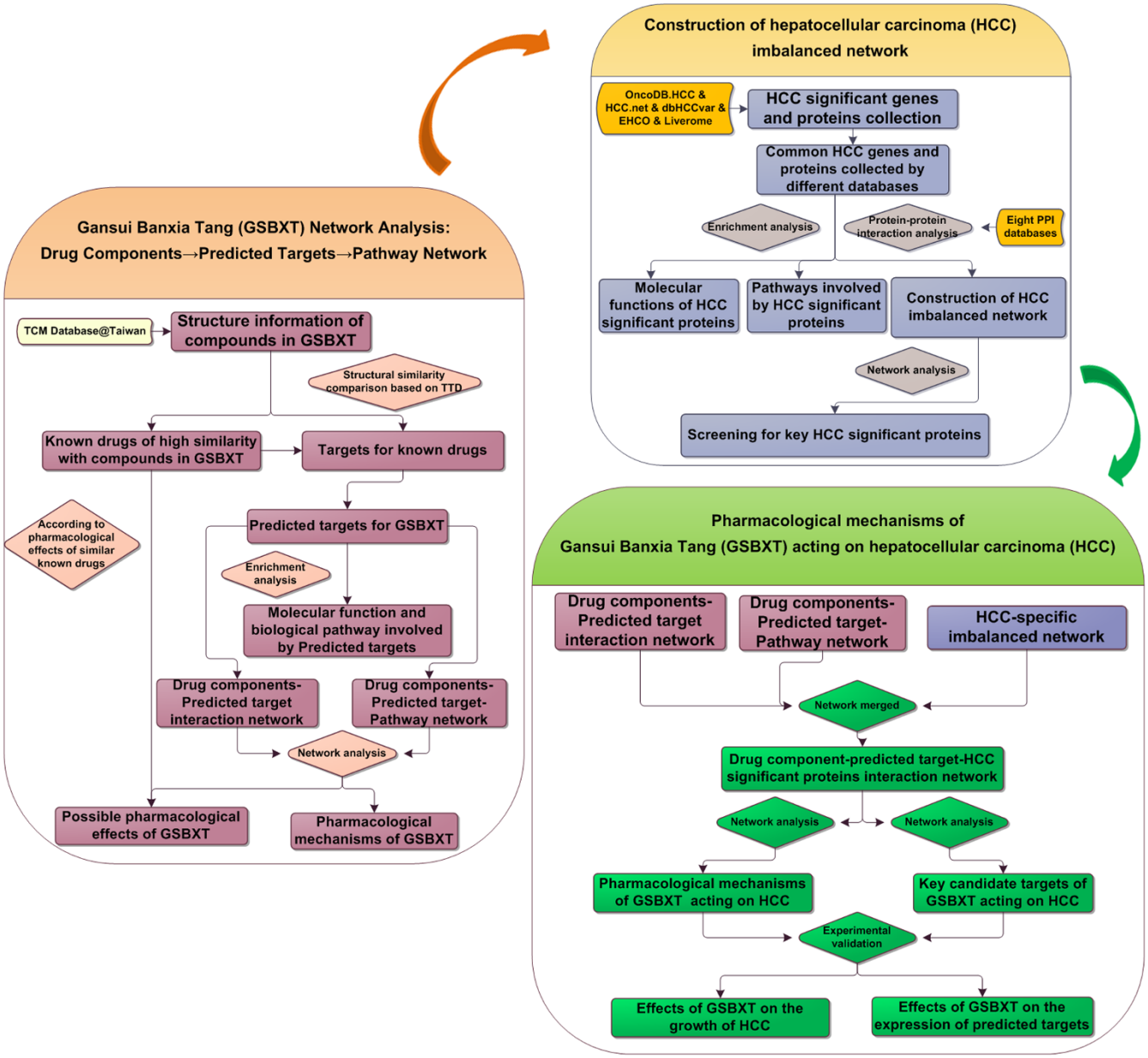

Figure 1 | A schematic diagram of this systems biology-based investigation into the pharmacological mechanisms of GSBXT acting on Hepatocellular carcinoma (HCC) by integrating multitarget identification and network analysis.

Putative target PPI network. Then, we constructed the putative target PPI network in order to evaluate the importance of putative targets in biological network. PPI data between putative targets and other proteins were collected from existing PPI databases (as described in 'Materials and methods' section). As shown in Figure 3A, the network consists of 1845 nodes (containing 48 putative targets marked with red ring) and 2985 edges. Four topological features, 'Degree,' 'Betweenness', 'Closeness' and 'K value' (defined in 'Materials and methods' section), were chosen to identify major putative targets. Totally, we identified 33 major putative targets, the 'Degree', 'Betweenness', 'Closeness' and 'K value' of which were all larger than the corresponding median values. Please see detailed information on topological features of 33 major putative targets in PPI network in Supplementary Table S3.

Ingredient-chemical component-major putative target-candidate HCC target network. To further clarify pharmacological mechanisms of GSBXT acting on HCC, we constructed Ingredient-major putative target-candidate HCC target network, which contains 364 nodes (including 5 ingredients and 33 major putative targets of GSBXT, and 326 candidate HCC targets) and 7647 edges as shown in Figure 3B. Of 33 major putative targets, 21 had more than 10 direct interactions with candidate HCC targets. Among them, 16 and 5 were major putative targets of Radix Kansui and Radix Glycytthizae, respectively, suggesting that the two medicines might play a principal role in the prevention of HCC, and other three medicines serve as adjuvant ones to assist the effects of the principal ingredients. Interestingly, the anti-HCC effects of Radix Kansui and Radix Glycytthizae have been reported by previous studies. For example, He et al. demonstrated that Radix Glycyrrhizae polysaccharide could reduce the proportion of Treg cells and up-regulate Th1/Th2 cytokine ratio in serum in H22 hepatocarcinoma bearing mice, which might partially cause the inhibition of tumor growth[17]; Yu et al. found the cytotoxic and antitumour activity of an octadecenoic acid extract, mainly containing oleic and linoleic acids, from Radix kansui on HCC cell line (BEL-7402)[19].

Table 1 | List of the putative targets for various chemical components containing in five ingredients of GSBXT

Putative Targets	NO. of Components*	Drug Ingredients
ACHE	2	Mel/Radix Glycytthizae
CHRNA2	1	Mel
CHRM1	7	Mel/Radix Glycytthizae/Radix Kansui
CHRM2	1	Mel
CHRM3	1	Mel
CHRM5	1	Mel
ADRB1	6	Radix Glycytthizae/Radix Kansui
ADRB2	1	Radix Glycytthizae
ALB	1	Raidix Paeoniae Alba
NAGLU	1	Radix Glycytthizae
AR	4	Radix Glycytthizae
ATP1A1	4	Raidix Paeoniae Alba/Radix Glycytthizae
SERPINA6	6	Raidix Paeoniae Alba/Radix Glycytthizae
BCHE	3	Radix Glycytthizae/Mel
CLCN2	1	Radix Glycytthizae
COMT	1	Radix Glycytthizae
CPT1A	1	Mel
CPT1B	1	Mel
DGAT1	1	Radix Glycytthizae
ESR1	1	Radix Glycytthizae
FCGR2A	6	Radix Glycytthizae/Radix Kansui
FGFR2	2	Raidix Paeoniae Alba/Radix Glycytthizae
FNTA	6	Radix Glycytthizae/Radix Kansui
ABAT	6	Radix Glycytthizae/Radix Kansui
GABRA1	6	Radix Glycytthizae/Radix Kansui
NR3C1	8	Raidix Paeoniae Alba/Radix Glycytthizae
HBA1	1	Raidix Paeoniae Alba
HBB	1	Raidix Paeoniae Alba
HMGCR	1	Raidix Paeoniae Alba
Hsp90α	6	Radix Glycytthizae/Radix Kansui
NR3C2	5	Radix Glycytthizae
MGAM	1	Radix Glycytthizae
MPI	1	Radix Glycytthizae
MLNR	3	Radix Glycytthizae
MTOR	3	Radix Glycytthizae
NOS2	1	Radix Glycytthizae
OPRD1	1	Radix Glycytthizae
OPRM1	6	Radix Glycytthizae/Radix Kansui
PLA2G1B	5	Radix Glycytthizae
PARP1	1	Rhizoma Pinelliae
PROC	1	Raidix Paeoniae Alba
RARA	1	Radix Glycytthizae
SLC12A1	7	Raidix Paeoniae Alba/Radix Glycytthizae/Radix Kansui
SCN5A	2	Raidix Paeoniae Alba
STAT3	6	Radix Glycytthizae
TUBB2C	2	Radix Glycytthizae
TBB5	9	Radix Glycytthizae
TOP2A	1	Radix Glycytthizae
TOP2B	1	Radix Glycytthizae
TRPA1	1	Radix Kansui
TRPM8	1	Radix Kansui
VDR	8	Raidix Paeoniae Alba/Radix Glycytthizae/Radix Kansui
WEE1	6	Radix Glycytthizae/Radix Kansui

Note: '*' refers to the number of the chemical components targeting the given putative targets.

Experimental validation. *GSBXT inhibits tumor growth in vivo*. To investigate whether GSBXT affects tumor growth in vivo, we applied a murine xenograft model of HepG2 cells. The low, middle and high dose groups were treated with GSBXT 3.6 g/kg, 7.2 g/kg and 14.4 g/kg daily p.o., respectively, and the control group received equal volume of saline solution per day. During the treatment, animal weight was not significantly different between the groups at any time point (Supplementary Figure S3). Meanwhile, according to the hematoxylin-eosin (H&E) stain, no toxic effects were observed in brain, heart, lung, liver or kidney (see Supplementary Figure S4). Moreover, GSBXT 7.2 g/kg and 14.4 g/kg administration could efficiently inhibit tumor growth in vivo as compared with the control group (Figure 4A). The tumor size and tumor weight of xenografts treated with 7.2 g/kg and 14.4 g/kg GSBXT were both significantly smaller than xenografts from the control group (all $P < 0.05$, Figure 4B and C).

Validation of the major putative targets of GSBXT. Among 21 major putative targets of GSBXT on HCC therapy, Hsp90α (HS90A_HUMAN), ATP1A1 (AT1A1_HUMAN) and STAT3 (STAT3_HUMAN) have most direct interactions with candidate HCC targets (50, 48 and 41 PPIs, respectively), suggesting that these three proteins might play important roles in the treatment of HCC. Therefore, we would like to illustrate their biological significance in HCC therapy as

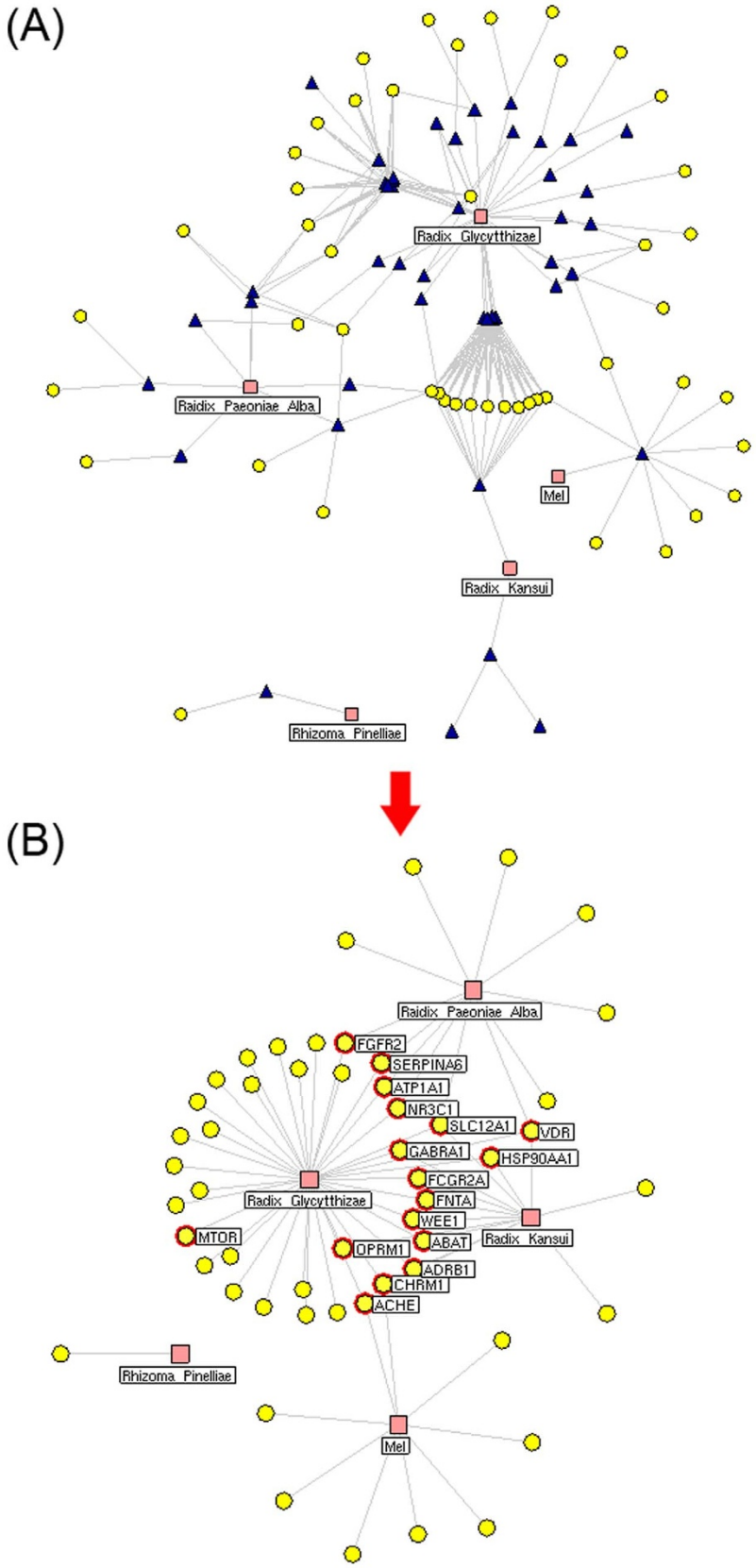

Figure 2 | Interaction network between chemical components of GSBXT and their putative targets built and visualized with Navigator. (A) Multi-level network of Ingredient-chemical component-putative target; (B) Interaction network of Ingredient-putative target extracted from (A), in order to understand relationships among drug ingredients in GSBXT. Edges: interactions between chemical components of GSBXT and their putative targets; Pink square nodes: five ingredients in GSBXT, including Radix Kansui, Rhizoma Pinelliae, Radix Glycytthizae, Raidix Paeoniae Alba and Mel; Blue triangular nodes: chemical components of GSBXT; Yellow round nodes: putative targets for chemical components of GSBXT. Yellow round nodes with red rings: putative targets shared by various ingredients in GSBXT.

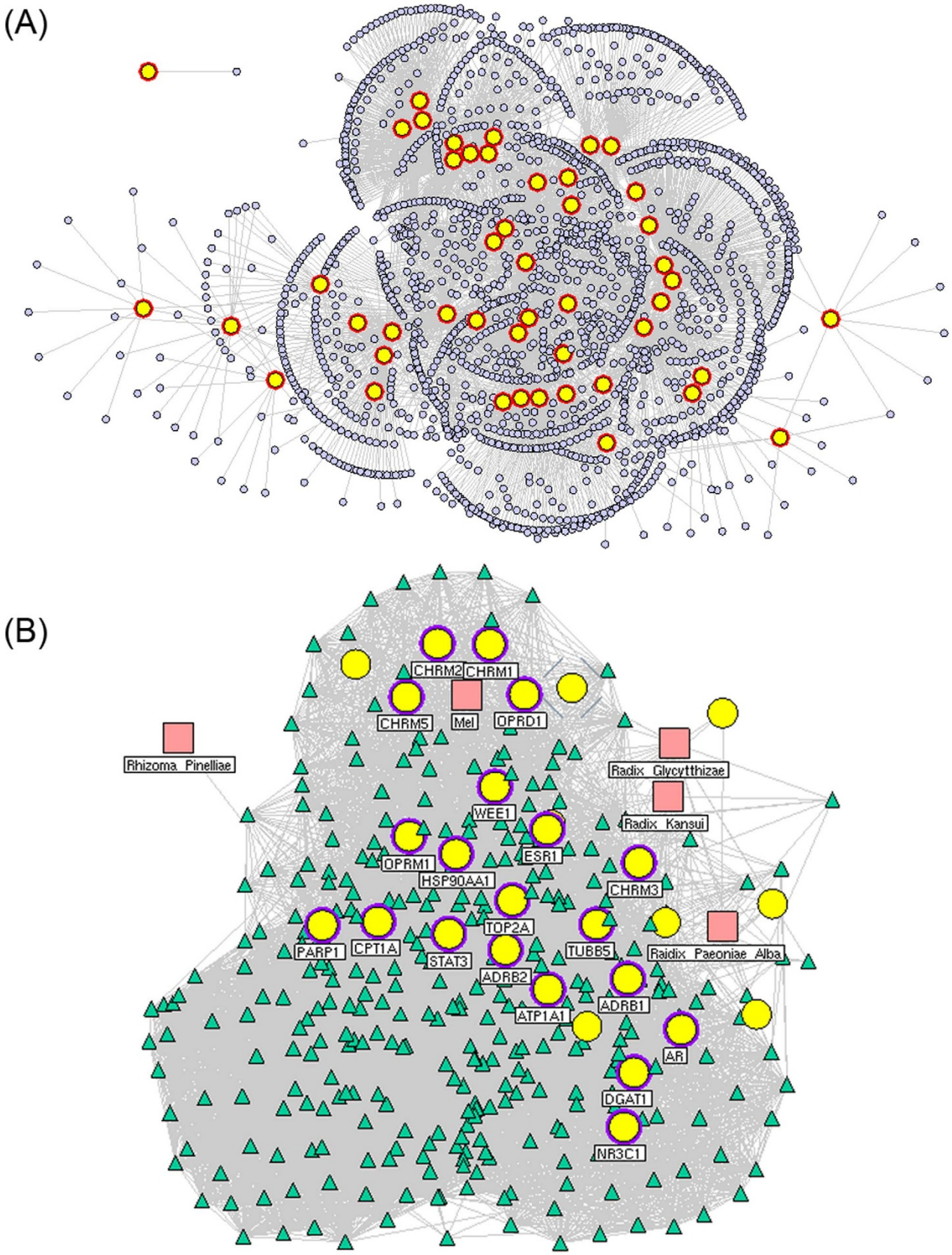

Figure 3 | (A) Protein-protein interaction (PPI) network between putative targets of GSBXT and their interactive partners built and visualized with Navigator. Edges: PPIs between putative targets of GSBXT and their interactive partners; Yellow round nodes: putative targets of GSBXT; Purple.round nodes: interactive partners of putative targets of GSBXT. (B) Multi-level network of drug ingredients → major putative targets → candidate HCC targets built and visualized with Navigator. Pink square nodes: five ingredients in GSBXT: Radix Kansui, Rhizoma Pinelliae, Radix Glycytthizae, Raidix Paeoniae Alba and Mel; Yellow round nodes: major putative targets of GSBXT; Yellow round nodes with purple ring: major putative targets which had more than 10 direct interactions with candidate HCC targets; Green triangular nodes: candidate HCC targets.

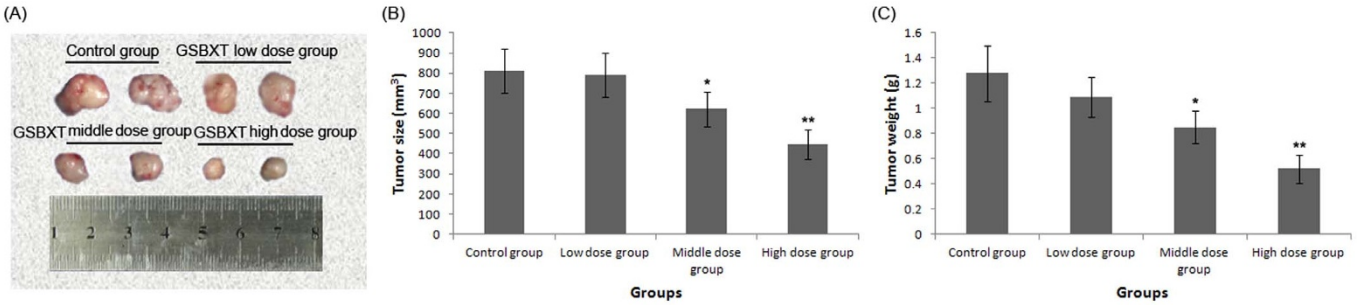

Figure 4 | GSBXT inhibits tumor growth in vivo. (A) Images of dissected tumors in control, low dose, middle dose and high dose groups. (B) Tumor sizes of xenografts in control, low dose, middle dose and high dose groups. (C) Tumor weight of xenografts in control, low dose, middle dose and high dose groups. Data are represented as the mean ± S.D. '*' and '**', $P < 0.05$ and $P < 0.01$, respectively, comparison with the control group.

described in Supplementary File S1. As shown in Figure S5 ~ S7, the PPI partners of Hsp90α, ATP1A1 and STAT3 are more frequently involved in various cancer related signal pathways. We further detected the changes into Hsp90α, ATP1A1 and STAT3 protein expression in tumor tissues of murine xenograft models with or without GSBXT administration in order to evaluate the influence of GSBXT in the three putative targets. The expression patterns and subcellular localizations of Hsp90α, ATP1A1 and STAT3 proteins in tumor tissues were examined by immunohistochemistry analysis. As shown in Figure 5A, Hsp90α protein was located in cytoplasm of tumor cells. With the treatment of GSBXT (doses of 3.6 ~ 14.4 g/kg), the immunoreactivity of Hsp90α protein was significantly reduced (low dose group vs. control group: 4.00 ± 1.73 vs. 8.00 ± 1.73, $P < 0.05$; middle dose group vs. control group: 2.00 ± 1.00 vs. 8.00 ± 1.73, $P < 0.01$; high dose group vs. control group: 0.67 ± 0.58 vs. 8.00 ± 1.73, $P < 0.001$; Figure 5A). Regarding to ATP1A1 protein, the positive immunoreactivity was observed on the cell membrane of tumor cells in each group (Figure 5B). Compared with the control group, ATP1A1 protein level in the tumor tissues of murine xenograft models treated with 7.2 ~ 14.4 g/kg GSBXT was dramatically reduced (middle dose group vs. control group: 2.33 ± 1.53 vs. 7.00 ± 1.73, $P < 0.01$; high dose group vs. control group: 0.33 ± 0.28 vs. 7.00 ± 1.73, $P < 0.001$, Figure 5B). Moreover, Figure 5C shown that STAT3 protein was localized in nuclear of tumor tissues. The statistic analysis found that the expression level of STAT3 protein in tumor tissues with the treatment of GSBXT (doses of 7.2 ~ 14.4 g/kg) was significantly lower than that in the control group (middle dose group vs. control group: 4.00 ± 2.00 vs. 8.00 ± 0.73, $P < 0.05$; high dose group vs. control group: 1.33 ± 0.58 vs. 8.00 ± 0.73, $P < 0.001$, Figure 5C). Similarly, Hsp90α, ATP1A1 and STAT3 protein expression levels detected by western blot analysis were also suppressed by doses of 7.2 ~ 14.4 g/kg GSBXT treatments significantly with a dose-dependent tendency (all $P < 0.05$, Figure 5D).

Accumulating studies have demonstrated that Hsp90α, ATP1A1 and STAT3 proteins may be upregulated in HCC, and the inhibition of these proteins may effectively retard the growth of HCC[22–24]. Thus, we speculate that GSBXT might play a role in suppressing tumor aggressive progression of HCC by targeting Hsp90α, ATP1A1 and STAT3 proteins.

Conclusion

Systems biology and network pharmacology are opening up the possibility to understand the multiple targets of ingredients in TCM formula and their interactions in the context of molecular networks. In the current study, we conducted a systems-level investigation combined with network analysis and experimental validation for pharmacological mechanisms of GSBXT on reversing HCC imbalanced network. Our results show as following:

(1) HCC imbalanced network was constructed using PPI data of HCC significant genes and proteins, which were differentially expressed or have genetic variations in HCC. Analysis on this disease-specific imbalanced network enables us to sufficiently utilize the gene co-expression information, which is believed to be more informative than expression changes of individual genes for target gene identification. In addition, network analysis is a powerful tool to understand pathological mechanisms of disease. By integrating the topological features of biological network, a list of candidate HCC targets were identified.

(2) The putative targets of five ingredients in GSBXT were predicted, which provides clues to investigate the pharmacological mechanisms of this formula for the treatment of HCC.

(3) The pharmacological network of GSBXT was build according to the relationships among ingredients, chemical components and putative targets, which provides insights into the synergetic effects of ingredients in this formula.

(4) Multilevel network with combination of HCC imbalanced network and pharmacological network of GSBXT has been build and can pinpoint out the key players of this formula acting on HCC and the corresponding putative targets.

(5) Bioinformatics integrated with experimental validation may provide an efficient and credible method to clarify the complicated multitargets mechanism for Chinese herbal formula.

However, the analysis favored well-studied genes and proteins, because the published literature-based primary interconnections were key criteria used to build the network. Thus, the current model might not be as effective for identifying orphan genes that function as central hubs in the network.

Taken together, this study developed a comprehensive systems approach of integrating disease-specific and drug-specific networks, and successfully explained the pharmacological mechanisms of GSBXT on reversing the HCC imbalanced network for the first time. Meanwhile, further experimental validation also demonstrated the preventive effects of GSBXT on tumor growth in mice and its regulatory effects on potential targets.

Methods

Data preparation. *Structural information of chemical components of each ingredient in GSBXT.* Structural information (*.mol or *.sdf files) of the chemical components of each ingredient in GSBXT were obtained from TCM Database@Taiwan23 (http://tcm.cmu.edu.tw/, Updated in Jun 28, 2012), which is currently the largest non-commercial TCM database worldwide. In total, we collected the structural information of 4 compounds for Radix Kansui, 13 compounds for Rhizoma Pinelliae, 82 compounds for Radix Glycytthizae, 15 compounds for Raidix Paeoniae Alba and 3 compounds for Mel.

HCC-significant gene and protein selection. HCC-significant genes and proteins were collected from five HCC related databases, including OncoDB.HCC (Last modified on Apr. 2008, http://oncodb.hcc.ibms.sinica.edu.tw/index.htm), HCC.net (Update time: Apr 18, 2010, http://www.megabionet.org/hcc/index.php), dbHCCvar (Last modified on Sep 4, 2012, http://genetmed.fudan.edu.cn/dbHCCvar/), EHCO (Encyclopedia of Hepatocellular Carcinoma genes Online, Last modified on Sep, 2012, http://ehco.iis.sinica.edu.tw), and Liverome (Last modified on Apr 14, 2011, http://liverome.kobic.re.kr/). For HCC-related molecular events, OncoDB.HCC is

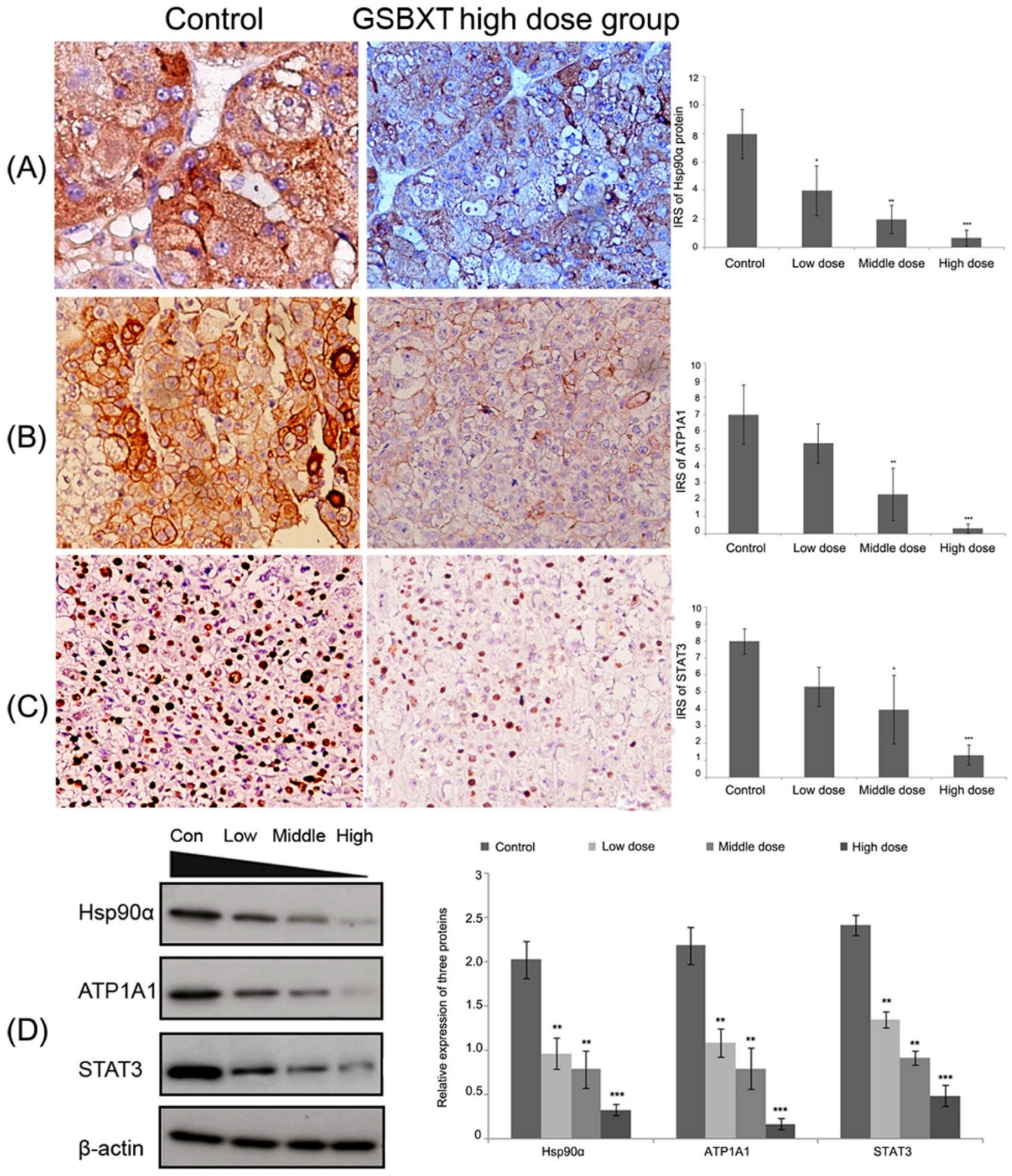

Figure 5 | GSBXT administration suppresses Hsp90α (A), ATP1A1 (B) and STAT3 (C) protein expression in tumor tissues of murine xenograft models examined by immunohistochemistry (A ~ C) and western blot (D). Data are represented as the mean ± S.D. '*', '**' and '***', $P < 0.05$, $P < 0.01$ and $P < 0.001$, respectively, comparison with the control group.

the first comprehensive HCC oncogenomic database and contains 577 HCC-related genes[24]. HCC.Net, which has compiled a network with thousands of HCC-related genes identified in different types and stages of HCC, contains 2,131 HCC-related genes[25]. dbHCCvar is an online database which contains 636 human genetic variations and 195 human genes which have been statistically tested to be associated with HCC[26]. EHCO is derived from thirteen gene sets related to HCC and gives 3833 HCC-significant genes[27]. Liverome is a curated database containing 6024 liver cancer-related gene signatures obtained mostly from published microarray and proteomic studies, and thoroughly curated by experts[28]. In order to facilitate data analysis, the different ID types for HCC significant genes and proteins were converted to ID from UniProtKB-Swiss-Prot.

Protein-protein interaction (PPI) data. PPI data were imported from eight existing PPI databases including Human Annotated and Predicted Protein Interaction

Database (HAPPI)[29], Reactome[30], Online Predicted Human Interaction Database (OPHID)[31], InAct[32], Human Protein Reference Database (HPRD)[33], Molecular interaction Database (MINT)[34], Database of Interacting Proteins (DIP)[35], and PDZBase[36]. The detailed information on these PPI databases is described in Supplementary Table S3. In order to facilitate data analysis, the different ID types for proteins from different PPI databases were converted to ID from UniProtKB-Swiss-Prot.

Pharmacological mechanism analysis. *Screening of similar drugs and prediction of putative targets for GSBXT.* As our previous study[20], we used Drug Similarity Search tool in Therapeutic Targets Database[37] (TTD, http://xin.cz3.nus.edu.sg/group/cjttd/ttd.asp, Version 4.3.02 release on Aug 25th 2011) to screen similar drugs of GSBXT through the structural similarity comparison. We only selected the drugs with high similar score (>0.85, similar ~ very similar) in the comparison with the structures of compositive compounds of each ingredient in GSBXT. The therapeutic targets of these similar drugs were also collected as putative targets of GSBXT. In total, we obtained 117 similar drugs and 53 putative targets of GSBXT. The detailed information on these similar drugs and putative targets is described in Supplementary Table S3. The performance of this prediction method has been evaluated in our previous study[20].

Gene Ontology (GO) and pathway enrichment analysis for HCC significant proteins and putative targets of GSBXT. We used Database for Annotation, Visualization and Integrated Discovery[38] (DAVID, http://david.abcc.ncifcrf.gov/home.jsp,version 6.7) for GO enrichment analysis. We also performed pathway enrichment analysis using pathway data obtained from the FTP service of KEGG[39] (Kyoto Encyclopedia of Genes and Genomes, http://www.genome.jp/kegg/, Last updated: Oct 16, 2012).

Network construction and analysis. The ingredients, chemical components, and putative targets of GSBXT, and HCC significant proteins were respectively used to construct ingredient-chemical component-putative target network, putative target PPI network, HCC significant protein PPI network (HCC imbalanced network) and ingredient-chemical component-putative target-candidate HCC target network. The PPI data were obtained from eight existing PPI databases as mentioned above. Then, we applied Navigator software (Version 2.2.1) and Cytoscape (Version 2.8.1) to visualize the networks.

HCC imbalanced network. The PPIs between HCC significant proteins and other human proteins were used to construct HCC imbalanced network. According to the previous study of Li et al.[21], we identified a node as a hub protein if its degree is more than 2 fold of the median degree of all nodes in a network. Then, the PPIs among hub HCC significant proteins were used to construct the network of hub HCC significant proteins. Moreover, four topological features, 'Degree', 'Betweenness', 'Closeness' and 'K value' (defined in 'Defining features set' section), were chosen to identify candidate HCC targets, the values of the four features for which were higher than the corresponding median values.

GSBXT ingredient-chemical component-putative target network. The ingredient-chemical component-putative target network was constructed by linking five ingredients containing GSBXT, the chemical components containing in all ingredients and their putative targets.

GSBXT putative target PPI network. The PPIs between all putative targets of GSBXT and other human proteins were used to construct GSBXT putative target PPI network. Similar with the analysis of HCC imbalanced network, the major putative targets were identified according to their values of the four topological features ('Degree', 'Betweenness', 'Closeness' and 'K value') in GSBXT putative target PPI network.

GSBXT ingredient-chemical component-major putative target-candidate HCC target network. GSBXT ingredient-chemical component-major putative target-candidate HCC target network was constructed by linking five ingredients containing GSBXT, the chemical components containing in all ingredients, their major putative targets and candidate HCC targets which were interacted with putative targets.

Defining features set. For each node i in the above networks, we defined four measures for assessing its topological property: (1) 'Degree' is defined as the number of links to node i; (2) 'Betweenness' is defined as the number of edges running through node i. (3) 'Closeness' is defined as the inverse of the farness which is the sum of node i distances to all other nodes. The Closeness centrality can be regarded as a measure of how long it will take to spread information from node i to all other nodes sequentially. Degree, betweenness and closeness centralities can measure a protein's topological importance in the network. The larger a protein's degree/betweenness/closeness centrality is, the more important the protein is in the PPI network[40]. (4) K-core analysis is an iterative process in which the nodes are removed from the networks in order of least-connected[41]. The core of maximum order is defined as the main core or the highest k-core of the network. A k-core sub-network of the original network can be generated by recursively deleting vertices from the network whose degree is less than k. This results in a series of sub-networks that gradually reveal the globally central region of the original network. On this basis, 'K value' is used to measure the centrality of node i.

Experimental validation. Nude mouse xenograft assays were used to examine the effects of GSBXT on the growth of HCC and to validate the predicted targets (HS90A_HUMAN, AT1A1_HUMAN and STAT3_HUMAN).

GSBXT preparation. The GSBXT used in this study is manufactured by Institute of Chinese Materia Medica, China Academy of Chinese Medical Sciences (Beijing, China) using five Chinese herbs at a composition of 1.5 g Radix Kansui, 9 g Rhizoma Pinelliae, 10 g Radix Glycytthizae, 15 g Raidix Paeoniae Alba, and 15 g Mel. Briefly, the Mel was mixed with all Radix Kansui, Rhizoma Pinelliae, Radix Glycytthizae, and Raidix Paeoniae Alba, follow by extraction with hot water (twice, 2 hr each). The representative chemical compositions of ephedrina hydrochloridum (0.00056%), adenosine (0.000684%), uridnine (0.0028%), trigonelline (0.0001152%), peoniflorin (0.053%), albiflorin (0.15%), glycyrrhizin (0.14%), glycyrrhizic acid (0.38%), liquiritigenin (0.015%), isoliquiritin (0.01%), and isoliquiritigenin (0.0019%) in GSBXT were determined by HPLC analysis.

Murine xenograft model & treatments. The experimental protocol was approved by Medical Experimental Animal Care Committee of 302 hospital of PLA and Institute of Chinese Materia Medica, China Academy of Chinese Medical Sciences.

Twenty 6-week-old male BALB/c-nude mice were obtained from SLRC Laboratory Animal (Shanghai, China). All mice were bred in laminar flow cabinets under specific pathogen-free conditions. Human HepG2 cells (1×10^8) were injected subcutaneously into the subaxillary space of each mouse. After that, all mice were randomly assigned to 4 groups (n = 5 for each group), which received a daily oral dose of vehicle solution (control group), 3.6 g/kg (low dose group, p.o. daily), 7.2 g/kg (middle dose group, p.o. daily) and 14.4 g/kg (high dose group, p.o. daily) GSBXT, respectively. The dose of GSBXT was based on human therapeutic dose. The recommended daily human dosage of GSBXT is 0.8 g/kg. According to the surface area rule, dosage of 7.2 g/kg is chosen as clinical equivalent dose in present study. The drugs were given with oral administration once daily for 21 consecutive days. Mice were weighed and the tumor width (W) and length (L) were measured every three days. Tumor volume was estimated according to the standard formula $1/2 \times L \times W^2$. Two days after the last administration, the animals were anesthetized. For each group, tumor tissues of three randomly selected mice were homogenized into tumor lysis buffer for western blot analysis. Tumor tissues of the other two mice were fixed in paraformaldehyde overnight for immunohistochemical analysis. Brain, heart, lung, liver and kidney tissues of three randomly selected mice were fixed in paraformaldehyde overnight for hematoxylin–eosin stain to detect the toxic effect of GSBXT.

Western blot assay. Western Blot procedures were described in our previous studies[42,43]. Primary antibodies included anti-Hsp90α (#ab59459, Abcam; Cambridge, MA), anti-ATP1A1 (#ab7671, Abcam; Cambridge, MA), anti-STAT3 (#ab15523, Abcam; Cambridge, MA), and anti-β-actin (#ab14128, Abcam; Cambridge, MA). All experiments were done in triplicate. Mean normalized protein expression ± SE was calculated from independent experiments.

Immunohistochemical staining. The immunohistochemical staining protocol and semiquantitative analysis were carried out following the protocol of our previous study[44]. Primary antibodies included anti-Hsp90α (#ab59459, Abcam; Cambridge, MA), anti-ATP1A1 (#ab7671, Abcam; Cambridge, MA) and anti-STAT3 (#ab15523, Abcam; Cambridge, MA).

Following a hematoxylin counterstaining, immunostaining was scored by two independent experienced pathologists, who were blinded to the background information of the mice. The scores of the two pathologists were compared and any discrepant scores were trained through re-examining the stainings by both pathologists to achieve a consensus score. The number of positive-staining cells in ten representative microscopic fields was counted and the percentage of positive cells was calculated. The percentage scoring of immunoreactive tumor cells was as follows: 0 (0%), 1 (1–10%), 2 (11–50%) and 3 (>50%). The staining intensity was visually scored and stratified as follows: 0 (negative), 1 (weak), 2 (moderate) and 3 (strong). A final immunoreactive score (IRS) was obtained for each case by multiplying the percentage and the intensity score.

Statistical analysis. The software of SPSS version13.0 for Windows (SPSS Inc, Chicago, IL, USA) and SAS 9.1 (SAS Institute, Cary, NC) was used for statistical analysis. Continuous variables were expressed as $\overline{X} \pm s$. For comparisons of means among multiple groups, one-way ANOVA followed by LSD test was performed. Differences were considered statistically significant when P was less than 0.05.

1. Parkin, D. M. *et al.* Global cancer statistics, 2002. *CA Cancer J. Clin.* **55**, 74–108 (2005).
2. Sherman, M. Recurrence of hepatocellular carcinoma. *N. Engl. J. Med.* **359**, 2045–2047 (2008).
3. Thorgeirsson, S. S. & Grisham, J. W. Molecular pathogenesis of human hepatocellular carcinoma. *Nat. Genet.* **31**, 339–346 (2002).
4. Forner, A., Llovet, J. M. & Bruix, J. Hepatocellular carcinoma. *Lancet.* **379**, 1245–1255 (2012).
5. Li, R. *et al.* Imbalanced network biomarkers for traditional Chinese medicine Syndrome in gastritis patients. *Sci. Rep.* **3**, 1543; doi:10.1038/srep01543 (2013).
6. Hyodo, I. *et al.* Nationwide survey on complementary and alternative medicine in cancer patients in Japan. *J. Clin. Oncol.* **23**, 2645–2654 (2005).

7. Swarup, A. B. *et al.* The use of complementary and alternative medicine by cancer patients undergoing radiation therapy. *Am. J. Clin. Oncol.* **29**, 468–473 (2006).
8. Ezeome, E. R. & Anarado, A. N. Use of complementary and alternative medicine by cancer patients at the University of Nigeria Teaching Hospital, Enugu, Nigeria. *BMC Complement Altern. Med.* **7**, 28 (2007).
9. Liao, Y. H. *et al.* Utilization pattern of traditional Chinese medicine for liver cancer patients in Taiwan. *BMC Complement Altern. Med.* **12**, 146 (2012).
10. Li, X. *et al.* Traditional chinese medicine in cancer care: a review of controlled clinical studies published in chinese. *PLoS One.* **8**, e60338 (2013).
11. Li, M. *et al.* Application of traditional Chinese medicine injection in treatment of primary liver cancer: a review. *J. Tradit. Chin. Med.* **32**, 299–307 (2012).
12. Wang, G. Z. & Li, H. C. Application of GSBXT in treatment of fluid retention. *J. Handan Med. College.* **10**, 182–183 (1997). In Chinese.
13. Song, W. Q. Utilization pattern of GSBXT in clinics. *J. Tradit. Chin. Med.* **34**, 492 (1993) In Chinese.
14. Yu, F. R. *et al.* Isolation and characterization of methyl esters and derivatives from Euphorbia kansui (Euphorbiaceae) and their inhibitory effects on the human SGC-7901 cells. *J. Pharm. Pharm. Sci.* **8**, 528–535 (2005).
15. Chen, L. In vitro Experimental Study of the Effect of Euphorbia kansui Extract on Human BEL-7402. *Acta BOt. Boreal. Occident. Sin.* **28**, 1889–1892 (2008). In Chinese.
16. Xia, B. Application of GSBXT in treatment of liver cancer. *Shanxi J. Tradit. Chin. Med.* **5**, 24 (1989) In Chinese.
17. He, X. *et al.* Down-regulation of Treg cells and up-regulation of TH1/TH2 cytokine ratio were induced by polysaccharide from Radix Glycyrrhizae in H22 hepatocarcinoma bearing mice. *Molecules.* **16**, 8343–8352 (2011).
18. Wang, Z. H. Application of GSBXT in treatment of esophageal cancer. *Tianjin med. onco.* **5**, 24 (1989) In Chinese.
19. Yu, F. *et al.* Cytotoxic activity of an octadecenoic acid extract from Euphorbia kansui (Euphorbiaceae) on human tumour cell strains. *J. Pharm. Pharmacol.* **60**, 253–259 (2008).
20. Zhang, Y. *et al.* A systems biology-based investigation into the pharmacological mechanisms of Wu Tou Tang acting on rheumatoid arthritis by integrating network analysis. *Evid. Based Complement Alternat. Med.* **2013**, 548498 (2013).
21. Csermely, P. *et al.* Structure and dynamics of molecular networks: a novel paradigm of drug discovery: a comprehensive review. *Pharmacol Ther.* **138**, 333–408 (2013).
22. Li, S. *et al.* Understanding ZHENG in traditional Chinese medicine in the context of neuro-endocrine-immune network. *IET Syst. Biol.* **1**, 51–60 (2007).
23. Chen, C. Y.-C. TCM Database@Taiwan: The World's Largest Traditional Chinese Medicine Database for Drug Screening In Silico. *PLoS ONE* **6**, e15939 (2011).
24. Su, W. H. *et al.* OncoDB.HCC: an integrated oncogenomic database of hepatocellular carcinoma revealed aberrant cancer target genes and loci. *Nucleic Acids Res.* **35(Database issue)**, D727–D731 (2007).
25. He, B. *et al.* HCCNet: an integrated network database of hepatocellular carcinoma. *Cell Res.* **20**, 732–734 (2010).
26. Yu, X. J. *et al.* dbHCCvar: a comprehensive database of human genetic variations in hepatocellular carcinoma. *Hum. Mutat.* **32**, E2308–E2316 (2011).
27. Hsu, C. N. *et al.* Detection of the inferred interaction network in hepatocellular carcinoma from EHCO (Encyclopedia of Hepatocellular Carcinoma genes Online). *BMC Bioinformatics.* **8**, 66 (2007).
28. Lee, L. *et al.* Liverome: a curated database of liver cancer-related gene signatures with self-contained context information. *BMC Genomics* **12(Suppl 3)**, S3 (2011).
29. Chen, J. Y. *et al.* HAPPI: an online database of comprehensive human annotated and predicted protein interactions. *BMC Genomics.* **10 Suppl 1**, S16 (2009).
30. Matthews, L. *et al.* Reactome knowledgebase of human biological pathways and processes. *Nucleic Acids Res.* **37**, D619–D622 (2009).
31. Brown, K. R. & Jurisica, I. Online predicted human interaction database. *Bioinformatics.* **21**, 2076–2082 (2005).
32. Aranda, B. *et al.* The IntAct molecular interaction database in 2010. *Nucleic Acids Res.* **38**, D525–D531 (2010).
33. Keshava Prasad, T. S. *et al.* Human Protein Reference Database – 2009 update. *Nucleic Acids Res* **37**, D767–D772 (2009).
34. Ceol, A. *et al.* MINT, the molecular interaction database: 2009 update. *Nucleic Acids Res.* **38**, D532–D539 (2010).
35. Lehne, B. & Schlitt, T. Protein-protein interaction databases: keeping up with growing interactomes. *Hum. Genomics.* **3**, 291–297 (2009).
36. Beuming, T. *et al.* PDZBase: a protein-protein interaction database for PDZ-domains. *Bioinformatics.* **21**, 827–828 (2005).
37. Zhu, F. *et al.* Therapeutic target database update 2012: a resource for facilitating target-oriented drug discovery. *Nucleic Acids Res.* **40**, D1128–D1136 (2012).
38. Dennis, G. Jr. *et al.* DAVID: Database for Annotation, Visualization, and Integrated Discovery. *Genome Biol.* **4**, P3 (2003).
39. Wixon, J. & Kell, D. The Kyoto encyclopedia of genes and genomes--KEGG. *Yeast.* **17**, 48–55 (2000).
40. Wang, Y. *et al.* Drug target prediction based on the herbs components: the study on the multitargets pharmacological mechanism of qishenkeli acting on the coronary heart disease. *Evid. Based Complement Alternat. Med.* **2012**, 698531 (2012).
41. Wuchty, S. & Almaas, E. Evolutionary cores of domain co-occurrence networks. *BMC Evol. Biol.* **5**, 24 (2005).
42. Liu, C. *et al.* Triptolide Prevents Bone Destruction in the Collagen-Induced Arthritis Model of Rheumatoid Arthritis by Targeting RANKL/RANK/OPG Signal Pathway. *Evid. Based Complement Alternat. Med.* **2013**, 626038 (2013).
43. Zhang, Y. *et al.* MicroRNA-101 suppresses SOX9-dependent tumorigenicity and promotes favorable prognosis of human hepatocellular carcinoma. *FEBS Lett.* **586**, 4362–4370 (2012).
44. Guo, X. *et al.* L1 cell adhesion molecule overexpression in hepatocellular carcinoma associates with advanced tumor progression and poor patient survival. *Diagn. Pathol.* **7**, 96 (2012).

Acknowledgments

This study was supported by the National Natural Science Foundation of China (no. 81303153) & the National Basic Research Program of China (973 Program) (2011CB505300, 2011CB505305).

Author contributions

L.Z. and L.N. participated in study design and coordination, material support for obtained funding, and supervised study. Z.Y. and G.X.: performed most of the experiments and statistical analysis and drafted the manuscript. W.D., L.R., L.X. and L.Y.: carried out the experiment and sample collection. X.Y., L.Z. and S.Z.: carried out the HPLC analysis. All authors reviewed and approved the final manuscript.

Additional information

Supplementary information accompanies this paper at http://www.nature.com/scientificreports

Competing financial interests: The authors declare no competing financial interests.

How to cite this article: ZHANG, Y.Q. *et al.* A systems biology-based investigation into the therapeutic effects of Gansui Banxia Tang on reversing the imbalanced network of hepatocellular carcinoma. *Sci. Rep.* **4**, 4154; DOI:10.1038/srep04154 (2014).